



ORIGINAL ARTICLE

# 3 Tesla MRI surface coil: Is it sensitive for prostatic imaging??



Mahmoud Agha <sup>a,b,\*</sup>, Ahmed Fathi Eid <sup>c</sup>

<sup>a</sup> Medical Research Institute, Alexandria University, Egypt

<sup>b</sup> Almana General Hospital, Saudi Arabia

<sup>c</sup> National Guard Hospital, Saudi Arabia

Received 22 October 2013; accepted 24 December 2013

Available online 30 January 2014

## KEYWORDS

MRI prostate;  
3 Tesla;  
Surface coil;  
Endocavitary coil;  
PSA;  
TRUS guided biopsy

**Abstract Objective:** This study aimed to check the sensitivity of phased array surface coils of 3T MRI, in pre-sampling diagnosis of prostate cancer, in an attempt to use it instead of endorectal coil. **Patients and methods:** This was a prospective comparative study, included 20 male patients, presented with suspected prostate cancer due to unexplained high PSA. The study protocol was approved by the ethics committee in Al-Mana General Hospital.

**Results:** Prostate cancer was correctly diagnosed by T2w sequence within 9 patients, 10 by DW&T2w, 13 by T2w – DW-DCE and 14 by of T2w-DW-DCE-MRS sequences.

**Conclusion:** 3T MRI imaging using phased array surface coil is a useful diagnostic tool for detecting prostate cancer, trustworthy when compared to endorectal approach.

© 2014 Alexandria University Faculty of Medicine. Production and hosting by Elsevier B.V. All rights reserved.

**Abbreviations:** ADC, apparent diffusion coefficient; BPH, benign prostatic hyperplasia; DCE-MRI, dynamic contrast enhanced MRI; DWI, diffusion-weighted MRI; 3dFES, 3d fastfield echo sequence; EPI, echoplanar imaging; ERC, endorectal coil; MRS, MR spectroscopy; NPV, negative predictive value; PACS, Picture archiving and communication system

\* Corresponding author at: P.O. Box 50367, Al Salhiyah, 12–14 Al Najah St., Al Ahsa, Hofuf 31982, Saudi Arabia. Tel.: +966 3; fax: +966 3 5887005.

E-mail addresses: [mahmoudagha23@hotmail.com](mailto:mahmoudagha23@hotmail.com), [dr.mahmoudagha@gmail.com](mailto:dr.mahmoudagha@gmail.com) (M. Agha), [fathieid@yahoo.com](mailto:fathieid@yahoo.com) (A.F. Eid).

Peer review under responsibility of Alexandria University Faculty of Medicine.

## 1. Introduction

Newly published international statistics had stated that prostate cancer is gaining remarkable increased records. World-wide surveys reported that among six men, one will be diagnosed as prostate cancer, during his lifetime. It is well known that such neoplasm occurs mainly in older men; about two thirds are diagnosed after the age of 65, it is uncommon before age 40. Age of 67 is considered average age at the time of diagnosis. It is considered the second leading cause of cancer death in American men, following bronchial carcinoma; about 1 man in 36 will die of prostate cancer.<sup>1</sup>

### 1.1. Risk factors for prostate cancer

Some factors might be associated with increased risk of prostate cancer, although such link is not yet clearly explained.

### 1.1.1. Age

Prostate cancer is very rare in men younger than 40, but the chance of having prostate cancer rises rapidly after age 50. Almost 2 out of 3 prostate cancers are found in men over the age of 65.

### 1.1.2. Race/ethnicity

Prostate cancer occurs more often in African-American men than in men of other races. African-American men are also more likely to be diagnosed at an advanced stage, and are more than twice as likely to die of prostate cancer as white men. Prostate cancer occurs less often in Asian-American and Hispanic/Latino men than in non-Hispanic.

### 1.1.3. Family history

Prostate cancer seems to be of high incidence in some families, which suggests that there may be an inherited or genetic factor. Having a first degree relative with prostate cancer doubles the risk of developing such disease. Also, the risk is much higher for men with several affected relatives.

### 1.1.4. Genes

Some inherited genes had been found to raise the risk for more than some type of cancer. For example, inherited mutations of the BRCA1 or BRCA2 genes are the reason that breast and ovarian cancers are much more common in some families. Mutations in these genes may also increase prostate cancer risk in some men, but they account for a very small percentage of prostate cancer cases.<sup>1-3</sup>

## 1.2. Clinical picture

The majority of prostate cancers are incidentally diagnosed in patients who are asymptomatic in the screening programs of prostate-specific antigen (PSA) level or findings on digital rectal examination. Some patients with prostate cancer may present with urinary complaints or retention, back pain, hematuria, frequency, urinary urgency, and decreased urine stream. However, these symptoms often result from benign prostatic hyperplasia (BPH).<sup>4,5</sup>

Manifestations of advanced disease result from combination of lymphatic, hematogenous, or contiguous local spread. Skeletal manifestations are especially common, because metastasis of prostate cancer has a strong osseous predilection. These advanced signs include weight loss and loss of appetite, anemia, bone aches, with or without pathologic fracture, and neurologic deficits from spinal cord compression. Also, lower extremity pain and edema due to obstruction of venous and lymphatic tributaries by nodal metastasis may be encountered. Uremic symptoms can occur from ureteral obstruction caused by local prostate growth or retroperitoneal adenopathy secondary to nodal metastasis.<sup>4,5</sup>

## 1.3. Pathophysiology

Adenocarcinoma is the most common type (95%). Approximately 4% of cases is transitional cell, which is thought to arise from the prostatic urethra epithelium. Squamous cell carcinomas constitute less than 1% of all prostate carcinomas. In many cases, prostate carcinomas with squamous

differentiation arise after radiation or hormone treatment. The few cases that have neuroendocrine morphology are believed to arise from the neuroendocrine stem cells normally present in the prostate. Of prostate cancer cases, 70% arise in the peripheral zone, 15–20% arise in the central zone, and 10–15% arise in the transitional zone. Most prostate cancers are multifocal, with synchronous involvement of multiple zones of the prostate.<sup>3,5</sup>

## 1.4. Diagnostic tools

### 1.4.1. Transrectal US (TRUS)

TRUS is usually the first applied imaging modality for diagnosis of prostate cancer. It can show the focal prostatic lesion and guide transrectal biopsy. Also, it can evaluate the layers of the rectal wall to determine the depth of tumor penetration and demonstrate the regional lymphadenopathy, if present. So, it can help in staging of prostate cancer, however as with all ultrasound examinations, it is operator dependent. There are many advantages that make TRUS the first and commonest applying imaging modality e.g. it is less expensive than magnetic resonance imaging (MRI); it is portable and not time consuming. Also, TRUS is well-tolerated by patients, and involves no radiation exposure.<sup>6,7</sup>

### 1.4.2. CT scan

CT scan has almost no role in the initial diagnosis of prostate cancer, due to poor tissue contrast between the prostate and the surrounding levator ani. Also, the prostatic spatial resolution is of limited value, so its internal anatomy is not well demonstrated. The major role of CT is in the nodal staging of prostate cancer, so that CT should be performed only in patients with a PSA level greater than 20, when it is possible to have advanced malignancy with nodal deposits. CT sensitivity for diagnosis of nodal deposits ranges around 36%, because of the missed microscopic ones. One of the benefits of CT scan is its high sensitivity, as guiding imaging modality in nodal biopsy. Also, CT scan is sensitive for early detection of osseous deposits, long before X-ray can do.<sup>8,9</sup>

### 1.4.3. Radionuclide bone scanning

Scintigraphy still remains the examination of choice for diagnosis of prostatic osseous deposits, which are frequently encountered complication even in symptom free patients. Bone scan is not strictly indicated for patients with PSA below 10 ng/mL, this is because chances of a positive bone scan are less than 1%. The incidence of osseous deposits increases in conjunction with PSA level, becoming more than 50% if PSA level is above 50 ng/mL. Prostatic bony deposits are commonly osteoplastic showing avid tracer uptake; however the less commonly reported osteopenic type may reflect extensive damage to bone with little osteoblastic activity.<sup>9</sup>

### 1.4.4. MRI

MRI had been proven to be an important imaging tool in the diagnosis of prostate cancer. MRI shows clear a delineation of the prostate as well as its high spatial resolution quality as regards demonstration of the internal zonal anatomy. Thus, it can show clear anatomical differentiation between the peripheral and transitional zone. In addition, MRI also allows

functional assessment with techniques such as diffusion-weighted MRI (DWI), MR spectroscopy (MRS), and dynamic contrast enhanced MRI (DCE-MRI).

#### 1.4.5. Normal MRI prostate

The prostate gland extends from the bladder base to the urogenital diaphragm with inverted pyramid like configuration. The prostate can be divided into five zonal sectors: non-glandular anterior fibromuscular stroma, peripheral zone (70%), central zone (25%), transition zone (5%) and periurethral glandular tissue (thin rim). T2-weighted sequence is considered the most informative sequence as regards demonstration of this zonal anatomy. The signal intensities in the central and transition zones show relative hypointense signal in comparison with high signal peripheral zone, surrounded by a thin rim of low signal intensity representing the fibrous capsule. The anterior fibromuscular stroma has also low signal intensity.<sup>9,10</sup>

The transition and central zones show similar intensity, so, they could be only differentiated by their assumed location. The transition zone extends from the bladder neck anterosuperiorly toward the verumontanum posterolaterally, anterior to the urethra. Central zone bounds on the posterior surface of the transition zone and proximal urethra and encloses the ejaculatory ducts. The periurethral zone, transition zone and central zone are collectively called central gland. Also, linear signal voids are seen posterolateral to the capsule, representing neurovascular bundles. Newly introduced functional MRI sequences; namely Diffusion weighted image (DWI), MR spectroscopy (MRS) and dynamic contrast studies are being evaluated for accurate early diagnosis of prostatic carcinoma.<sup>9,10</sup>

## 2. Patients and methods

### 2.1. Study population

This is a prospective study which aims to check the sensitivity of phased array surface coils of 3T MRI, in pre-sampling diagnosis of prostate cancer in 20 consecutive patients. It was done in Almana General Hospital (AGH)-Eastern Province-KSA, where a newly introduced 3T MRI (Siemens-Magnetom Verio 3T-Siemens medical solution-Erlangen-Germany), which was used in this study. This study was done in an attempt to replace the commonly used endocavitary rectal coil with surface coil, which is more acceptable by patients, if proven to be of similar or nearby sensitivity.

Screening program with annual PSA test for all hospital male clients, above age of 50 was established many years ago in AGH. MRI followed by TRUS guided biopsy was routinely recommended for anyone who has age-specific unexplained elevated PSA. PSA level judgment was done, according to the international agreed standard normal values for different

age groups. Also MRI was done for any patient, regardless of his age group, with high PSA velocity i.e. rapid unexplained rising serum PSA level ( $> 0.4-0.75$  ng/ml/yr.)<sup>11</sup> Table 1.

Through OSRIX PACS system (Picture Archiving and Communication System), the DICOM images were transferred to and stored in mother computer, with high storage capacity. Access to these images can be easily done with RIS (radiology information system). Also, all laboratory findings, histopathological results, medical or surgical history if any were clearly reordered for all patients.

### 2.2. Technique

MRI examinations had been done using phased array surface coil with fixed sequence parameters. Sequences include coronal, sagittal and axial T2w and axial T1w sequences, dynamic contrast study (DCE-MRI 3D fastfield echo sequence (3DFES)), diffusion weighted images and MRS. In DCE, 0.1-mmol/kg bolus of Gadodiamide (Omniscan, GE Healthcare AS, Oslo, Norway) was administered at a rate of 1.5 mL/s followed by a 20-mL saline flush using a power injector. Images were acquired before contrast and at 30, 60, and 180 s after the contrast injection was initiated. Table 2.

DWI was obtained using EPI (echoplanar imaging) with single-shot free breathing sequence, utilizing proton water diffusion properties to produce image contrast, with b-values 0 and 1000 s/mm<sup>2</sup>, in an attempt to demonstrate the characteristic restricted diffusion of prostate cancer. MRS was done through water- and lipid-suppressed double spin-echo point-resolved spectroscopy (PRESS) sequence. Axial T2-weighted images were used as localizer, to select the PRESS volume aiming to maximize the coverage of the prostate while minimizing the inclusion of periprostatic fat and rectal air. The scan direction in the z-axis was angled anteriorly from (0° to 25°) following the anatomical orientation of the gland, in this direction. Careful target localization was usually attempted especially, in tumors at the periphery of the gland at the prostate-rectum and prostate-periprostatic fat interface. Table 2.

### 2.3. MRI analysis

The two consultant radiology authors reviewed the images of this study, first individually, and then dual discussion was made shortly after the separate evaluation. Results of T2w sequence alone were reordered first separately and then collectively in different combination groups that were divided according the other types of sequences added to the initial T2w sequence. So, results of the study were recorded under four different sequence combinations for efficacy comparison. These groups were T2w sequence results alone at first, then in combination with DWI results in the second group, DCE was added in the third and lastly MRS was added in the fourth. Table 3. These sequences are the most widely used MRI sequence for prostatic images, as published in many new literatures.<sup>9,10</sup>

Non contrast T1w sequences have regional compromised tissue contrast resolution, so it was only used to check for hemorrhage if any. In DCE sequences, the previously published literatures reported four different patterns of enhancement; no enhancement, gradual enhancement (slow wash in), early and prolonged enhancement (rapid wash-in, delayed washout)

**Table 1** Age specific normal PSA.

Age group (Years)	Normal PSA value (ng/ml)
50–60	3
60–70	4
70–80	5

**Table 2** MRI sequences parameters.

Sequence	TRTE (msec)	FOV(mm)	Matrix	Slice thickness(mm)	Flip angle
Axial T2w	2600/100	100	512 × 512	3	65
Coronal T2w	2600/100	100	512 × 512	3	90
Sagittal T2w	2800/100	100	512 × 512	3	90
Axial T1w	550/10	100	512 × 512	3	65
DCE-MRI (3DFES)	3.3/1.6	100	256 × 256	3	10
DWI (b value: 0–1000 s/mm <sup>2</sup> )	2800/80	30	128 × 128	3	90
MRS	1000/100	90	72 × 72	6	90 /180 /180 °

**Table 3** Diagnostic sensitivity percentages of the different sequence combinations.

Sequence	True +ve	True-ve	False +ve	False-ve	Sensitivity %	Specificity %	PPV%	NPV %
T2w	9	4	1	6	60	80	90	40
T2w + DW	10	4	1	5	66.6	80	90.9	44.4
T2w + DW + DCE	13	4	1	2	86.6	80	92.8	66.6
T2w + DW + DCE + MRS	14	5	0	1	93.3	100	100	83.3

and early shortly persistent enhancement (rapid wash-in & rapid washout). Rapid wash-in and early washout is the standard enhancement pattern of malignant prostatic tumors, while benign lesions usually show no or delayed wash-in as well as delayed washout enhancing pattern.<sup>12</sup>

On diffusion weighted images (DWI), malignancy was considered when lesions show obvious restricted diffusion, which is seen as hyperintense signal in DWI and hypointense signal in apparent diffusion coefficient (ADC). This sequence was applied in the three orthogonal planes with b-values of 0 and 1000 s/mm<sup>2</sup>.<sup>13,14</sup> In MRS, high choline/creatine levels and depletion of citrate level are the standard criteria of malignancy. The mean normal choline-creatine/citrate ratio is <0.5, it is considered suspicious for malignancy if >0.5 and very suspicious if >0.8.<sup>13</sup>

Results of the MRI were recorded in stamped sheets before availability of pathological results.

### 3. Results

Prostate cancer was correctly reported by T2w sequence within 9 patients (45%), 10 patients by combined interpretation of DW&T2w sequences (50%), 13 patients by combined T2w – DW- DCE (65%) and 14 patients by combination of T2w-DW-DCE-MRS sequences (70%). Correct exclusion of prostate cancer was made through T2w images in 4 patients (20%), by T2w and DWI in through T2w images in 4 patients (20%), by T2w, DWI and DCE images in 4 patients (20%), and T2w, DWI and DCE and MRS separately and in all other combinations in 5 patients (25%).

MRI examinations were incorrectly negative in 6 (30%), 5 (25%), 2 (10%) and only one patient (5%). Sensitivity of correct diagnosis was 60%, 66.6%, 86.6% and 93.3%. Specificity was 80%, 80%, 80% and 100%. Positive predictive value (PPV) was 90%, 90.9%, 92.8% and 100%. Negative predictive value (NPV) was 40%, 44.4%, 66.6% and 83.3%. These results were recorded in T2w alone, T2w + DWI, T2w + DW + DCE and T2w + DW + DCE + MRS,

respectively. Also, incorrect positive diagnosis of prostate cancer which had been excluded by biopsy was encountered in only one patient (5%) with T2w alone, T2w and DW together, and T2w + DW + DCE sequences. [Table 3](#). [Chart 1](#).

Pathological results of US guided transrectal biopsies were prostate cancer in 15 patients (75%), BPH in 3 patients (15%), and bacterial prostatitis in one patient (5%) and non-bacterial prostatitis in another one (5%). In these groups, the average PSA levels were 16.7, 5.4, 8.5, 6.7 ng/dl, respectively. [Table 4](#).

### 4. Discussion

MRI examination of the prostate gland was performed as per standard procedures through the use of endorectal coil (ERC) at 1.5 T MRI apparatuses, in an attempt to obtain a sufficiently high signal-to-noise ratio with subsequent good spatial resolution to allow clear demarcation of any prostatic focal lesion. The location, signal changes, pattern of growth and extension were the standard criteria for suggestion of the pathological diagnosis of prostatic swellings. At 3T MRI, considering increased magnet power, it is expected to have increased signal-to-noise ratio with body or surface phased array coils. So studies to check accuracy and sensitivity of imaging with these surface coils were in need to replace ERC which was not easily tolerated by considerable number of male patients.

Our study included 20 male patients (50–80y), who were clinically suspected to have prostate cancer due to lower urinary tract symptoms in combination with age group specific high PSA. We tried to apply all possible valuable sequences that may help increasing the sensitivity of diagnosis with such easily tolerated coils. MRI sequences that were applied in this study were T2w, DW, DCE and MRS, in different groups combination, namely T2w alone, T2w and DWI, T2w, DWI and DCE and lastly, all together. Criteria of diagnosis of prostate cancer in each sequence were carefully evaluated by the two radiology authors and compared with the standard imaging criteria of standard normal prostate MRI model. ([Fig. 1](#)).

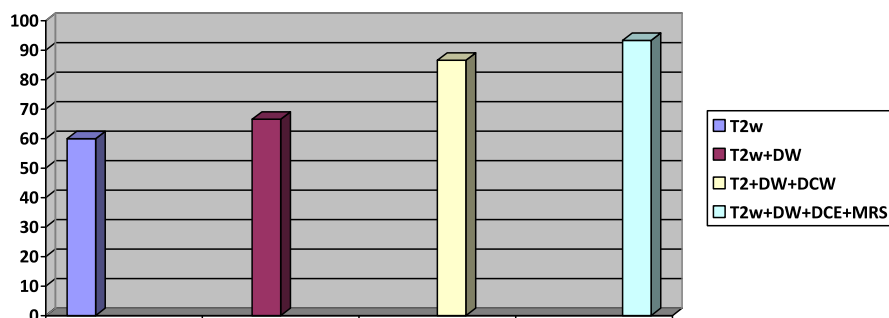


**Chart 1** Representation of different diagnostic sensitivity percentages of different sequences combination.

**Table 4** TRUS biopsy results with PSA average of the different groups.

Pathological diagnosis	No.	Average PSA ng/dl
Prostate cancer	15 (75%)	16.7
BPH	3 (15%)	5.2
Bacterial prostatitis	1 (5%)	8.5
Non-bacterial prostatitis	1 (5%)	6.7

Through T2W sequence alone, 9 cases of cancer were correctly diagnosed, while 4 cases were also correctly excluded. False positive results were recorded as one positive and 6 negative cases. These findings give records of 60% sensitivity, 80% specificity, 90% PPV and 40% NPV. This result could be explained by the variable diagnostic sensitivity of T2w images, according to regional location of the lesions. Peripheral zone cancer foci were clearly recognized as ill-defined low-signal-intensity lesions with or without extracapsular extension. This clear identification of malignant tumors in peripheral zone could be explained by the regional contrast difference between MRI signals of normal glandular tissue and malignant tissue. Peripheral zone of prostate, which comprises 70–80% of the glandular tissue, exhibits diffuse homogenous intense bright signal in T2w sequence, due to high acinar and ductal fluid contents. So, compact non glandular malignant tissue which displays obvious T2w low signal could be easily localized at this peripheral zone in contrast to the normal high T2w signal. Fortunately more than 70% of prostate cancer develops at this zone, hence the importance of T2w sequence in diagnosis of prostate cancer.<sup>15</sup> (Fig. 2A and B) Also these recognized peripheral zone lesions were obviously documented by positive findings of these lesions in DWI and DCE images. (Fig. 2 C and D).

On the contrary, central and transitional zones display low or heterogeneous T2 signal intensity since due to fewer glandular structures and smooth muscles, so there is a clear demarcation between them and the peripheral zone with sharp interface, called pseudocapsule. However, central and transitional zones can not be differentiated from each other on top of MRI signal basis, only by assumed location of each lobe. Owing to their normal signal heterogeneity, tumors could not be clearly outlined by T2w sequence alone, hence the need for additional helpful MRI sequences. (Fig. 3A) This matches with what is described by Cheikh et al. in a study published in 2009 in European Radiology Journal.<sup>16</sup>

Diffusion-weighted MRI (DWI) has been implied for imaging of extra-cranial structures since the 1990s, due to the

advent of high resolution short sequences like echo-planar imaging (EPI). DW-MRI provides information about the molecular movement of water in biological tissues. Diffusion of water within the body is impeded by cell membranes, so the neoplastic compact cellular tissues significantly restrict the motion of extracellular water. DWI alone had a score of true positive diagnosis of 10 cases and true negative exclusion of 3 cases. Fallacious results of DWI were recorded as wrong negative exclusion of 5 cases and false positive diagnosis of 2 cases. This gives indices of 66.6% sensitivity, 60% specificity, 100% positive predictive value and 37.5% of negative predictive value.

Restricted diffusion in the three orthogonal planes was expressed as DWI high signal intensity in comparison of the low signal intensity of the normal prostatic tissue. However some overestimation of the restricted diffusion could be seen in issues with long T2 relaxation time, which is termed T2 shine through. This could be avoided through review of ADC map, which shows restricted diffusion as low signal intensity avoiding T2 shine through contamination. (Figs. 2C and 3B). So, such application of this short time sequence can correct some fallacious negative results of T2w images, alone at central zone. This also agrees with what was described by Kim in study published at June 2010 in American Journal of Roentgenology (AJR).<sup>17</sup>

Its short acquisition time makes it easy to be routinely included in prostate imaging protocols and also, it can help in early detection of tumor recurrence. It may help checking response for treatment and it can also guide biopsy intake from the most compact cellular part of the tumor. However, DWI has some limitations such as non-standardized ADC protocols, image distortion and susceptibility artifacts that may limit sensitivity of DWI especially in follow up studies for evaluation of the therapeutic responses. So application of more advanced software and hardware is needed to overcome such problems.<sup>17</sup> Also, DWI has some specificity limitation because of overlap between some compact cellular lesions of different pathology e.g. Some types of BPH and prostatitis may have altered cellular density and interstitial pressure, so they can mimic prostate cancer on DWI.<sup>18</sup>

Application of dynamic contrast enhanced MRI (DCE-MRI) intends to demonstrate the characteristic neoplastic new angiogenic effect, through demonstrating altered pattern of enhancement after contrast injection in tissues over short period of time. The enhancement intensity at ROI is expressed through post-processing workstation, as intensity-time curve chart. Angiogenic effect of neoplastic process leads to early enhancement and early washout of neoplastic tissue, rather

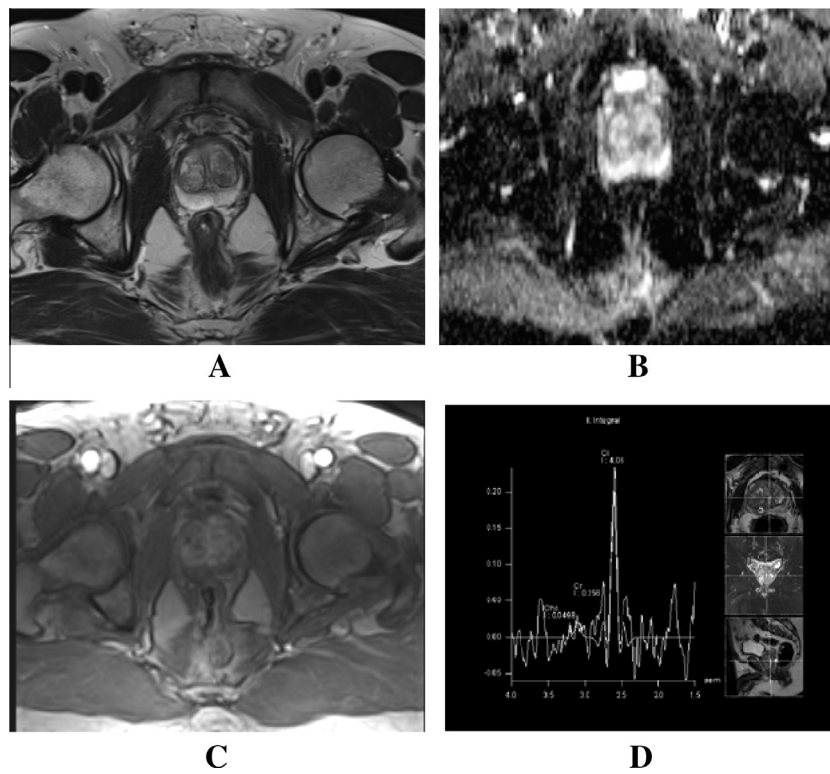


**Figure 1** Standard MRI of normal prostate. (A) T2w, (B) ADC, (C) DCE axial image and (D) MRS.

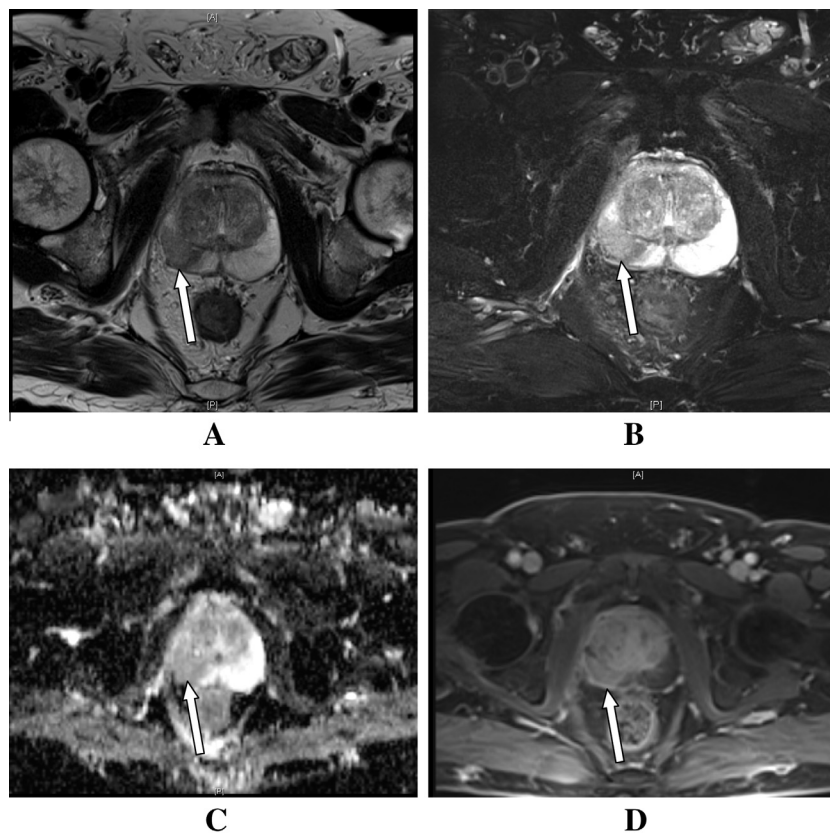


**Figure 2** (A) Axial T2w image and (B) Axial T2w Fat Sat. image show right sided peripheral zone unencapsulated hypointense lesion. (C) Axial ADC image shows significant diffusion restriction within the lesion. (D) Axial DCE arterial phase shows early avid enhancement of the swelling simulating the enhancement of the central zone. (Arrow)

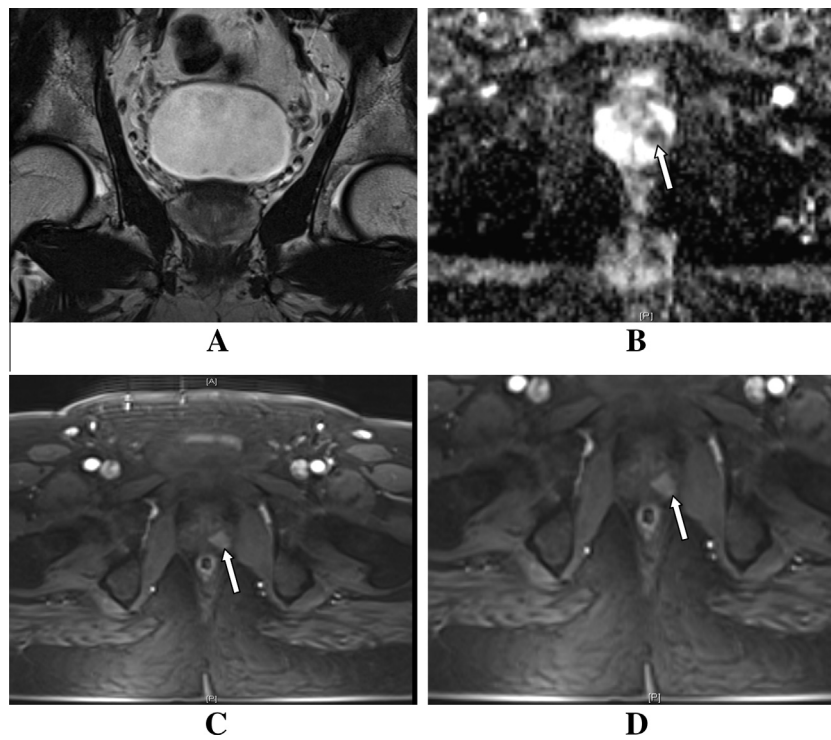


**Figure 3** Pathologically proven prostate cancer. (A) Coronal T2w image showing no masses in the central zone. (B) ADC axial image shows left paramedian central zone focal lesion with restricted diffusion. (C) DCE arterial phase axial images show early arterial enhancement of the lesion. (Arrow in B&C).

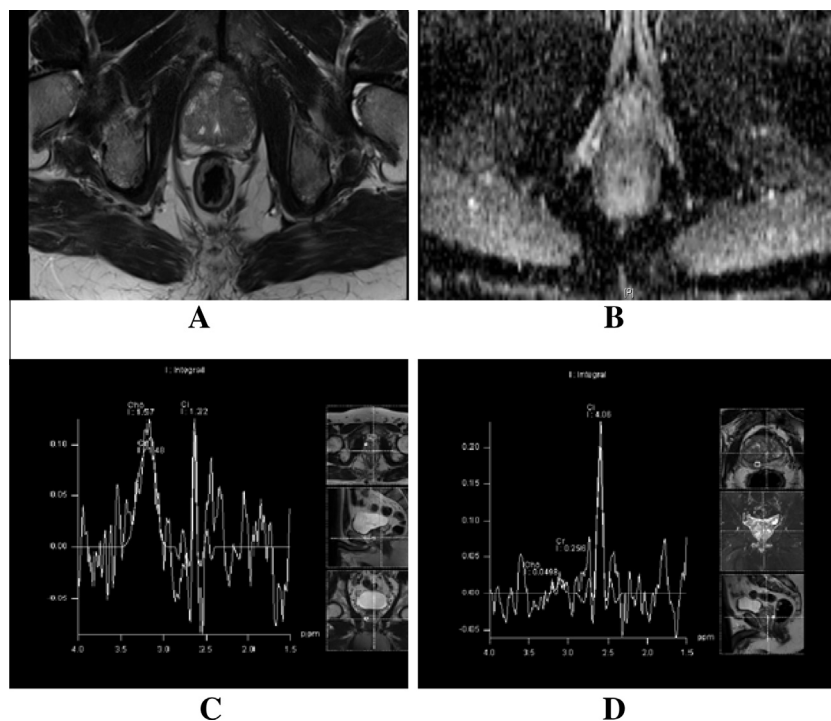


**Figure 4** (A) T2w and (B) ADC axial images show no abnormalities, while MRS (C) shows a severe rise in choline-creatine/citrate ratio (1.0) (characteristic MRS sign of malignancy) in comparison with the standard normal value (D).

than slowly enhanced and slowly washed normal tissue or benign lesions. (Fig. 2D and 3C and D).

In our study, DCE-MRI had lower scores than DWI and T2W, with records of 7 true positive, 3 true negative, 2 false

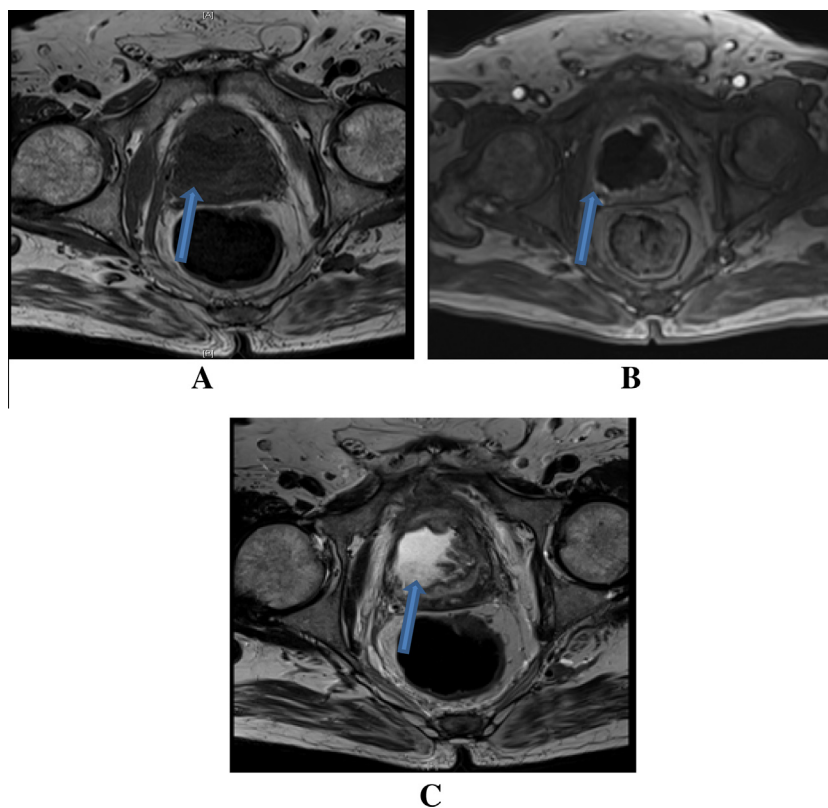


**Figure 5** (A) Axial non contrast T1w, (B) DCE Axial and (C) Axial T2w images show prostatic abscess as cystic central zone hypointense lesion in A, with postcontrast ring enhancement in B and fluid level in C. (Arrows).

positive and 8 false negative cases, 46.6% sensitivity, 60% specificity, 77.7% PPV and 27.2% NPV. This could be explained again by limited sensitivity of DCE-MRI in diagnosis of central zone lesions with missed some lesions, due to early regional normal tissue enhancement masking the neoplastic enhancement pattern. Also, it could not help in differentiating hypovascular malignant tumors from benign tumors, as both show slow or non-enhancement pattern. Some unavoidable technical errors- e.g. rectal motions- may distort the relatively long timed dynamic sequences, thus deforming the dynamic curve. Also, some benign prostatic lesions may show high vascularity, like some types of BPH, showing enhancement pattern of nearby criteria to the neoplastic enhancement curves. Similar findings were reported by Iwazawa in diagnostic and interventional radiology journals, at 2011.<sup>19</sup>

Application of point-resolved spectroscopy (PRESS) MRS for the targeted region of interest in the prostate results in correct diagnosis of 16 cases (11 positive and 5 negative) and false negative exclusion of 4 patients, with 73.3% specificity, 100% sensitivity, 100% PPV and 55% NPV. These results had raised the scores of sensitivity of MRI examinations using surface coils with 3 T MRI, relying upon demonstration of increased levels of specific metabolites formed by the neoplastic growth. The normal prostatic MRS shows high citrate and low choline-creatine spectra. Choline metabolite peak resonant spectrum is so close, commonly indistinguishable from the choline peak and expressed as one spectrum. Cancer cells utilize citrate oxidizing metabolism with high turnover of phospholipids raising the choline level and suppressing citrate level, thus there will be

increase the choline-creatine/citrate ratio more than 0.5<sup>13</sup> (Fig. 4).

The false negative results could be explained by the small in size of the lesions, so signals from surrounding normal tissues overlap the neoplastic signals. This agrees with study published by Verma S. in American Journal of Roentgenology (AJR) at June 2010.<sup>20</sup>

In summation of positive findings of T2w sequence, DWI, DCE-MRI and MRS, 3 Tesla MRI surface coil prostatic examination had achieved good scores of 93.3% sensitivity, 100% specificity, 100% PPV, 83% NPV. This score supported the fact that 3T MRI imaging of prostate using phase array surface coil is a useful diagnostic tool for detecting prostate cancer, trusty replacing endorectal approach which was the standard protocol for examinations done with 1.5 T. In addition to diagnosis of prostate cancer, this technique of MRI examination through these combined sequences had been also proven to have high sensitivity in diagnosis of non-malignant lesions, that may clinically and even laboratory simulate prostate cancer, e.g. prostatic abscess or prostatitis. (Fig. 5).

#### Limitation of the study

Due to recent installation of the 3 tesla MRI in our hospital, we had relatively small number of candidates suitable for this study (20 patients). However, we plan to expand the application of this MRI protocol in larger number of patients, on a longer term study in the nearby future.

**Conflict of interest**

None.

**References**

1. Patrick C. Walsh and Janet F. Worthington. Guide to Surviving Prostate Cancer (introduction: x–xiv). Second ed. June 27, 2007. Wellness Central. Hachette Book Group.
2. Giovannucci E, Liu Y, Platz EA, Stampfer MJ, Willett WC. Risk factors for prostate cancer incidence and progression in the health professionals follow-up study. *Int J Cancer* 2007;**121**(7):1571–8.
3. Razvan Bardan, Viorel Bucuras, Alis Dema, Mircea Botoca. Prostate Cancer: Epidemiology, Etiology, Pathology, Diagnosis and Prognosis. Timisoara 2007; 2–3 Part I: 225–32.
4. Horwich I A, Parker I C, Bangma C, Kataja V. Prostate cancer: ESMO Clinical Practice Guidelines for diagnosis, treatment and follow-up. *Ann Oncol* 2010;**21**(5):v129–33.
5. Epstein JI. Pathologic and clinical findings to predict tumor extent of nonpalpable (stage T1c) prostate cancer. *JAMA* 1994;**271**(5):368–74.
6. Bax J et al. “Mechanically assisted 3D ultrasound guided prostate biopsy system. *Med. Phys.* 2008 Dec;**35**(12):5397–410.
7. Real-time Contrast-enhanced Transrectal US-guided Prostate Biopsy: Diagnostic Accuracy in Men with Previously Negative Biopsy Results and Positive MR Imaging Findings. *Radiology*. 2013 269:1 159–166.
8. Johannes G, Korporaal, Cornelis AT, van den Berg, Jeukens Cécile RLPN, Greetje Groenendaal. Dynamic contrast-enhanced ct for prostate cancer: relationship between image noise, voxel size, and repeatability. *Radiology* 2010;**256**(3):976–84.
9. Hedvig Hricak, Choyke Peter L, Eberhardt Steven C, Leibel Steven A, Scardino Peter T. Imaging prostate cancer: a multidisciplinary perspective. *Radiology* 2007;**243**(1):28–53.
10. Boonsirikamchai Piyaporn, Choi Seungtaek, Frank Steven J, Ma Khaled M, Elsayes Khaled M, Kaur Harmeet, et al. MR Imaging of prostate cancer in radiation oncology: what radiologists need to know. *Radiographics* 2013;**33**(3):741–61.
11. François Cornelis, Gérald Rigou, Yann Le Bras, Xavier Coutouly, Regis Hubrecht, Mokrane Yacoub, Gilles Pasticier, Grégoire Robert, and Nicolas Grenier. Real-time Contrast-enhanced Transrectal US-guided Prostate Biopsy: Diagnostic Accuracy in Men with Previously Negative Biopsy Results and Positive MR Imaging Findings. *Radiology* October 2013 269:1 159–166.
12. Engelbrecht Marc R, Huisman Henkjan J, Robert Laheij JF, Jager Gerrit J, van Leenders Geert JLH, Hulsbergen-Van De Kaa Christina A. Discrimination of prostate cancer from normal peripheral zone and central gland tissue by using dynamic contrast-enhanced MR imaging. *Radiology* 2003;**229**(1):248–54.
13. Radswiki and Dr Paresh K Desai. MR spectroscopy in prostate cancer. <http://radiopaedia.org/articles/mr-spectroscopy-in-prostate-cancer>.
14. Chan Kyo Kim, Byung Kwan Park, Bohyun Kim. Diffusion-Weighted MRI at 3 T for the Evaluation of Prostate Cancer. *AJR* 2010; 194:1461–[146] ‘9.
15. Jackson ASN, Reinsberg SA, Sohaib SA, et al. Dynamic contrast-enhanced MRI for prostate cancer localization. *Br J Radiol* 2009;**82**:148–56.
16. Alexandre Ben Cheikh, Nicolas Girouin, Marc Colombel, et al. Evaluation of T2-weighted and dynamic contrast-enhanced MRI in localizing prostate cancer before repeat biopsy. *Eur Radiol* 2009;**19**:770–8.
17. Chan Kyo Kim, Byung Kwan Park, Bohyun Kim. Diffusion-weighted MRI at 3 T for the evaluation of prostate cancer. *AJR* 2010;**194**:1461–9.
18. Jin Iwazawa, Takashi Mitani, Seitaro Sassa, Shoichi Ohue. Prostate cancer detection with MRI: is dynamic contrast-enhanced imaging necessary in addition to diffusion-weighted imaging? *Diagn Inter Radiol* 2011;**17**:243–8.
19. Jin Iwazawa, Takashi Mitani, Seitaro Sassa, Shoichi Ohue. Prostate cancer detection with MRI: is dynamic contrast-enhanced imaging necessary in addition to diffusion-weighted imaging? *Diagnostic and interventional radiology (Ankara, Turkey)* 2011;**17**(3):243–8, #xB7.
20. Verma Sadhna, Rajesh Arumugam, Fütterer Jurgen, Turkbey Tom WJ, Scheenen Tom WJ, Pang Yuxi, Choyke Peter L, Kurha John. Prostate MRI and 3D MR Spectroscopy: How We Do It. *Am J Roentgenol* 2010;**194**:1414–26.